Computers and Mathematics with Applications 57 (2009) 1862–1868

Contents lists available at ScienceDirect

Computers and Mathematics with Applications

journal homepage: www.elsevier.com/locate/camwa

A universal texture segmentation and representation scheme based on ant colony optimization for iris image processing☆

Lin Ma [a,*], Kuanquan Wang [a], David Zhang [b]

[a] School of Computer Science and Technology, Harbin Institute of Technology, Harbin, 150001, China

[b] Department of Computing, Hong Kong Polytechnic University, Hunghom, Kowloon, Hong Kong

ARTICLE INFO

Keywords:
Ant colony optimization
Image segmentation
Iris image processing
Texture feature representation

ABSTRACT

This paper proposes a novel scheme for texture segmentation and representation based on Ant Colony Optimization (ACO). Texture segmentation and texture characteristic expression are two important areas in image pattern recognition. Nevertheless, until now, how to find an effective way for accomplishing these tasks is still a major challenge in practical applications such as iris image processing. We propose a framework for ACO based image processing methods. Considering the specific characteristics of various tasks, such a framework possesses the flexibility of only defining different criteria for ant behavior correspondingly. By defining different kinds of direction probability and movement difficulty for artificial ants, an ACO based image segmentation algorithm and a texture representation method are then presented for automatic iris image processing. Experimental results demonstrated that the ACO based image processing methods are competitive and quite promising, with excellent effectiveness and practicability especially for images with complex local texture situations.

1. Introduction

Iris is the only one so-called inner organ of the human body that is directly and easily visible with the naked eye. Because of its special physiology architecture, the iris becomes very sensitive to the status of all other organs and a healthy condition of the human body. From an anatomical point of view, the front 70% of the iris contains a large number of blood vessels, and various kinds of nerves spread all over the iris. Thus, the brain, nerve center and all other organs can transfer information directly to the iris; this makes the iris able to react quickly to changes in the inner hormone level and inner conditions, and produce visible changes of the iris's appearance such as pigmentation, freckles, appearance of white rings surrounding the cornea or sclera, broken texture, *etc*. [1,2] These facts make it a popular belief that systematic changes in the iris's pattern reflect the condition of organs in the body, one's mood or personality, *etc*.

Practitioners skilled in the art of interpreting these aspects of iris patterns for diagnosing people's health, personality, and mutual compatibilities, are called iridologists. Iridology is a novel approach of medical diagnosis, with such advantages as no touching, no damage, no paint and high precision. In European countries, the study of iridology has a history of nearly 100 years. Nowadays, both in Europe and America, researchers concentrate on studying the relationships between changes in the iris and diseases in human organs. Dr. Jensen had published a very detailed and well recognized iris chart showing how each individual organ of the body is connected to a specific spot on each iris. And iridologists popularly use

☆ This work was supported in part by the Specialty Leader Support Foundation of Harbin (2003AFLXJ006), the Foundation of Heilongjiang Province for Scholars Returned From Abroad (LC04C17), the NSFC No. 60571025 and the NSFC Key Oversea Project under the contract No. 60620160097.

* Corresponding author.
E-mail addresses: malin_li@hit.edu.cn (L. Ma), wangkq@hit.edu.cn (K. Wang), csdzhang@comp.polyu.edu.hk (D. Zhang).

0898-1221/$ – see front matter © 2008 Elsevier Ltd. All rights reserved.
doi:10.1016/j.camwa.2008.10.012

this chart for diagnosis. In the fields of computer science and artificial intelligence, people interest in applying the iris for automatic personal identification & verification and automatic healthy surveillance. To achieve such purposes, image processing technologies, especially image segmentation methods should be well studied.

Image segmentation is a traditional problem in digital image processing that involves partitioning an image into several disjoint regions. Each region should be homogeneous with respect to some specific properties [3,4]. It is a difficult problem, and no general solution has yet been formulated [5]. However, many good solutions have been proposed for specific classes of segmentation problems. Among such classes, the issue of segmenting textured images such as the iris image is particularly challenging. Many recent successful techniques have been based on multi-band filtering [6–9] or on purely stochastic models [10–15].

In this paper, we take a distinct approach by applying the ant colony optimization (ACO) idea to the iris image segmentation. With simulated annealing (SA), genetic algorithm (GA) and Tabu search (TS), ACO [16,17] is another typical meta-heuristic search algorithm applied in hard combinatorial optimization problems such as traveling salesman problems, graph coloring problems, quadratic assignment problems or vehicle routing problems, *etc*. The discretion and parallel nature of ACO are well suitable to digital images. The reason is that not only can ACO search smartly, but also have good characteristics such as robustness, positive feedback and distributed computation [18].

In our iris study, image segmentation is regarded as outlining the regions of pixels with a similar background texture. For each pixel in an image, its brightness and gradient, together with neighboring pixel's brightness and gradient are taken as local texture features. For ACO, the movement of artificial ants is influenced by these local texture features, and the global pheromone distribution on the image of a large number of artificial ants reveals the region segmentation and texture representation results. After segmentation, texture representation for some specific regions are compared between normal people and patients suffering the corresponding disease. Experimental results proved not only the effectiveness of ACO in image segmentation, but also proved the discriminatibility of the ACO based texture representation.

The present work is organized as follows: Section 2 gives an overview of related work in the area and propose a framework of ACO based image processing model. Section 3 describes two algorithms based on the proposed model, one for image segmentation and the other for texture representation. In Section 4 the experimental results are shown and its implications are discussed. Finally, Section 5 concludes the paper and suggests future research.

2. A framework of ACO based image processing methods

As we know, the ACO algorithm was firstly proposed by an Italian scholar, M. Dorigo [18]. Observing the behavior of real ants gathering food and discovering the best path from their nest to the destination, biologists found that: an individual ant is a simple creature whose activity appears to be random, disorganized and unmotivated. However, an ant colony is highly organized, complicated and efficient. Ants communicate through releasing a kind of chemical substance called a pheromone, and the detected intensity of the pheromone will affect ants' decision of choosing which direction to go. In such a way, ants are able to find the shortest path from the nest to a food source. Even if the conditions vary, an ant colony can also adjust their strategy to get a new shortest path. This substance influences the choices they make: the larger the amount of pheromone on a path, the higher the probability that an ant will select the path. The quantity of pheromone deposited will guide other ants moving to the path with strongest concentration of pheromone. This collective behavior of ant colony reveals a positive feedback of information. Cooperative interaction of ants leads to emergence of the shortest paths.

The inspiration of ACO came from such observations of real ants to solve discrete optimization problems. The research of ACO on digital images was proposed by Ramos and Almeida [19], and revealed that artificial ant colonies can react and adapt to any type of digital habitat [20]. To segment an image, feature distinctions between different parts inside the image must be found. There are many features of an image, such as object, background, edge, colors, *etc*. [21] proposed an algorithm for swarm-based color segmentation, where two specialized type of agents evolve over RGB images, and solutions to color segmentation problems emerge from the swarm behavior. [22] presents a study on the edge-detection of different gray-level images with artificial swarm intelligence, and concludes that artificial swarms can perform feature extraction in digital images. [23] presents an evolutionary swarm algorithm for image segmentation where different populations of individuals compete to occupy a bi-dimensional landscape representing the image to be processed.

Summarizing the main issues for an ACO, we propose a framework of ACO based image processing model as following. The idea is to introduce information about the problem into the decision making process and the pheromone releasing process of the artificial ants.

2.1. Artificial ant and its behavior

Assuming there is a large number of artificial ants wandering in their territory. The territory is considered as a toroidal bidimensional lattice, which is represented by an $M \times N$ cells territory array. At the beginning, each ant is randomly placed on a cell (x, y) in the territory array.

At each discrete time element thereafter, each ant moves to an adjacent location and reinforces the pheromone level on that spot. The model may have two different policies: one cell may be occupied by one and only one ant, or ants are allowed to share the same cell. In our study, we adopted the first policy and an ant will not move if it finds itself totally surrounded by others ants. This policy was proved to be more appropriate to evolve on digital images [19].

When an ant moves, it chooses a cell in the 8cellneighbor of the current location considering 2 factors: pheromone intensity and movement momentum. Regarding the movement momentum, a direction probability vector $P^{\text{dir}} = (p_1^{\text{dir}}, p_2^{\text{dir}}, \ldots, p_8^{\text{dir}})$ is defined, where p_i^{dir} represents the weight for the i-th candidate cell. The final transition probability for the i-th candidate cell is thus given by Eq. (2.1), where θ_i is the current pheromone intensity at the cell.

$$P_i = \frac{p_i^{\text{dir}}\theta_i^{\alpha}}{\sum_{j=1}^{8} p_j^{\text{dir}}\theta_j^{\alpha}} \quad (here: 1 \le i \le 8). \tag{2.1}$$

Here, α is a coefficient that balances the importance of the accumulated pheromone to the movement momentum factor. The value of α may be defined either experimentally or heuristically. To ACO, ants choose their next stay point c depending on the maximum transition probability: $c = argmax\{P_1, P_2, \ldots, P_8\}$. Clearly, different definitions of the movement momentum and the evolution of pheromone should fit the demands of various application problems.

2.2. Evolution of pheromone

Let $\theta_{(x,y)}$ stands for the pheromone intensity at the cell (x, y). At the beginning, each $\theta_{(x,y)}$ is assigned to zero for the whole territory array, $1 \le x \le M$, $1 \le y \le N$. Each time an ant visits a cell, it releases a constant amount η of pheromone, plus a dynamic amount $\varepsilon \cdot \Delta((x, y), (x_0, y_0))$, which is monotone to the difficulty of this movement. Here, ε is a constant, $\Delta((x, y), (x_0, y_0))$ expresses the difficulty of movement from the previous cell (x_0, y_0) to cell (x, y).

$$\theta_{(x,y)} \leftarrow \theta_{(x,y)} + \eta + \varepsilon \cdot \Delta((x, y), (x_0, y_0)). \tag{2.2}$$

In addition, during every iteration all cell's pheromone is decreased exponentially by a constant K, $0 < K < 1$. Thus, the evolution of pheromone is given by:

$$\theta_{(x,y)} \leftarrow K \cdot \theta_{(x,y)}. \tag{2.3}$$

2.3. Image habitat

To process an image for a specific purpose, the original image should be transformed into an image habitat in order to suit the artificial ants. Usually, an $M \times N$ pixels image is simply regarded as an $M \times N$ cells territory array. However, the dimension of the image may also be different from the territory array, thus lets ants realize an automatic image resolution transformation.

Concerning image features, different feature distinctions between different parts inside the image must be found. There are many features for an image, such as object, background, edge, color, *etc*. In an image application, we interest in those features to distinguish objects from the background, such as a gradient of pixels, local differences produced by various differential operators, differences of subimages, *etc*.

After constructing the image habitat, image segmentation based on an ant's behavior is the process that ants with different features search for food sources. Ants roam in an image and look for the pixels with largest pheromone under its movement momentum. When ants move to the boundary or pixels without a similar pheromone level, the ant's roaming will stop for the current iteration. After several iterations, ACO will converge. And the distribution of pheromone intensity reveals the marking results of the ant colony for segmentation.

3. ACO based algorithms for image segmentation and texture representation

Under the proposed framework, here we present two algorithms that aim at iris image segmentation and texture representation separately. The key points relating to the design of the direction probability vector P^{dir} and the movement difficulty $\Delta((x, y), (x_0, y_0))$.

3.1. ACO based image segmentation

As formerly described, image segmentation aims at partitioning an image into several homogeneous disjoint regions. We thus design mechanisms to emphasize the monotony of pixel gray level and local texture similarity. Moving under such supervision, ants tend to roam within homogeneous regions. And as a result, the pheromone intensity within each region appears to be monotone, and leaves a relatively lower pheromone intensity path between disjoint regions.

3.1.1. Direction probability vector definition

In other studies, direction probability vectors used to be determined in advance and stay unique during the whole ant movement process. Traditionally, an ant tends to maintain its movement direction, and weights for all directions are assigned according to the distortion between the candidate direction and the original direction. That is, if an ant comes from south, and the eight cells have no pheromone, the chance of going north is higher, followed by the chance of going northeast or northwest, an so on, until the likelihood of returning south, which is very low. In our work, we apply this mechanism as a

bias, but we also apply other 2 criteria to involve the landscape information. Thus our direction probability vector contains 3 parts as:

$$p_i^{\text{dir}} = p_i^1 + p_i^2 + p_i^3. \tag{3.1}$$

To make things simple, we numerate the 8 neighbor cells as: the 1st cell is the one where comes the ant, the others are counted clockwise. The 1st items p_i^1 for each p_i^{dir} is assigned by the vector $(\frac{1}{20}, \frac{1}{12}, \frac{1}{4}, \frac{1}{2}, 1, \frac{1}{2}, \frac{1}{4}, \frac{1}{12})$. Clearly, this part is the basic movement momentum.

The 2nd items p_i^2 is set according to the similarity of gray level between the i-th cell $f_{(i)}$ and the center cell $f_{(0)}$: $p_i^2 = \frac{1}{1+|f_{(i)}-f_{(0)}|^\beta}$. β is an experimentally chosen parameter to align these factors. Clearly, this part reflects the similarity among neighboring pixels. The more similar the gray level of the pixels, the more possible it is that the pixels belong to the same class.

The 3rd items p_i^3 is given by the local texture similarity between the sub-image $W_{(i)}$ which is extended from the i-th cell, and the center sub-image $W_{(0)}$: $p_i^3 = \frac{1}{1+|d(W_{(i)},W_{(0)})|^\gamma}$. γ is also an experimentally chosen balancing parameter. Here, the center cell with the 8 neighbors naturally form a 3×3 pixels sub-image $W_{(0)}$. Around $W_{(0)}$, there exit also 8 neighbors of 3×3 pixels sub-image: $W_{(1)}, W_{(2)}, \ldots, W_{(8)}$, which can be equally numerated in same way as that for neighboring cells. The distance between 2 sub-images $d(W_{(i)}, W_{(0)})$ may have many forms, however we simply apply the histogram distance. Clearly, this part reflects the similarity of gray level distribution in the neighboring sub-images. The more similar the distributions are, the higher the probability that the sub-images belong to the same class.

3.1.2. Movement difficulty definition

Usually, the gray level of an object is very different from that of background. In addition, edge points are generally points where gray values suddenly change. The gradient, which provides a measure of this change, is another important feature to distinguish edge point from the background or object region. Trying to reduce the pheromone intensity at edge cells, we let the movement difficulty to be the gray level gradient, and thus simply define $\Delta(i, 0) = A \cdot p_i^2$, where A is just a constant.

3.1.3. Procedure of algorithm

We have the following procedure to implement the proposed algorithm above, the Ant Colony Optimization Image Segmentation Algorithm (ACO-ISA).

- Step-1: Initialize parameters such as α, β, γ, K and A, *etc.*; initialize pheromone distribution $\theta_{(x,y)}$.
- Step-2: ***For*** all ants, ***do***: place each ant agent randomly on the territory array;
- Step-3: ***For*** $t = 1$ to T_{max}, ***do***: Step-4 to Step-12; here T_{max} controls the maximum iterations.
- Step-4: ***For*** all ants, ***do***: Step-5 to Step-10;
- Step-5: Compute global direction probabilities P_i, according to Eqs. (2.1) and (3.1).
- Step-6: Select the adjacent cell with the largest P_i.
- Step-7: ***If*** the selected cell is occupied by another ant, ***do***: continue for the next ant.
- Step-8: Move the ant.
- Step-9: Increase the pheromone at the cell according to Eq. (2.2).
- Step-10: Continue for the next ant.
- Step-11: Evaporate pheromone by K, at all cells according to Eq. (2.3).
- Step-12: Continue for the next iteration.
- Step-13: End.

3.2. ACO based texture representation

After the original image is partitioned into several regions, we proposed another ACO based method to represent the texture characteristics within each region. Different from the idea of segmentation, the idea of texture representation aims at expressing the visual texture. To achieve this goal, ants should become sensitive to local changes of gray levels, so the definition of the direction probability vector and the movement difficulty will change.

3.2.1. Direction probability vector definition

The general form for the direction probability vector rest the same as formula (3.1), and the 1st item p_i^1 stays unchanged. However, the 2nd items p_i^2 is now set to emphasize the difference of gray levels between the i-th cell $f_{(i)}$ and the center cell $f_{(0)}$: $p_i^2 = |f_{(i)} - f_{(0)}|^\beta$. The 3rd items p_i^3 is also given by the local texture difference between the i-th subimage $W_{(i)}$ and the center subimage $W_{(0)}$: $p_i^3 = |d(W_{(i)}, W_{(0)})|^\gamma$.

3.2.2. Movement difficulty definition

Trying to increase the pheromone intensity at edge cells according to texture changement, here we let $\Delta(i, 0) = B \cdot p_i^3$, where B is just a constant.

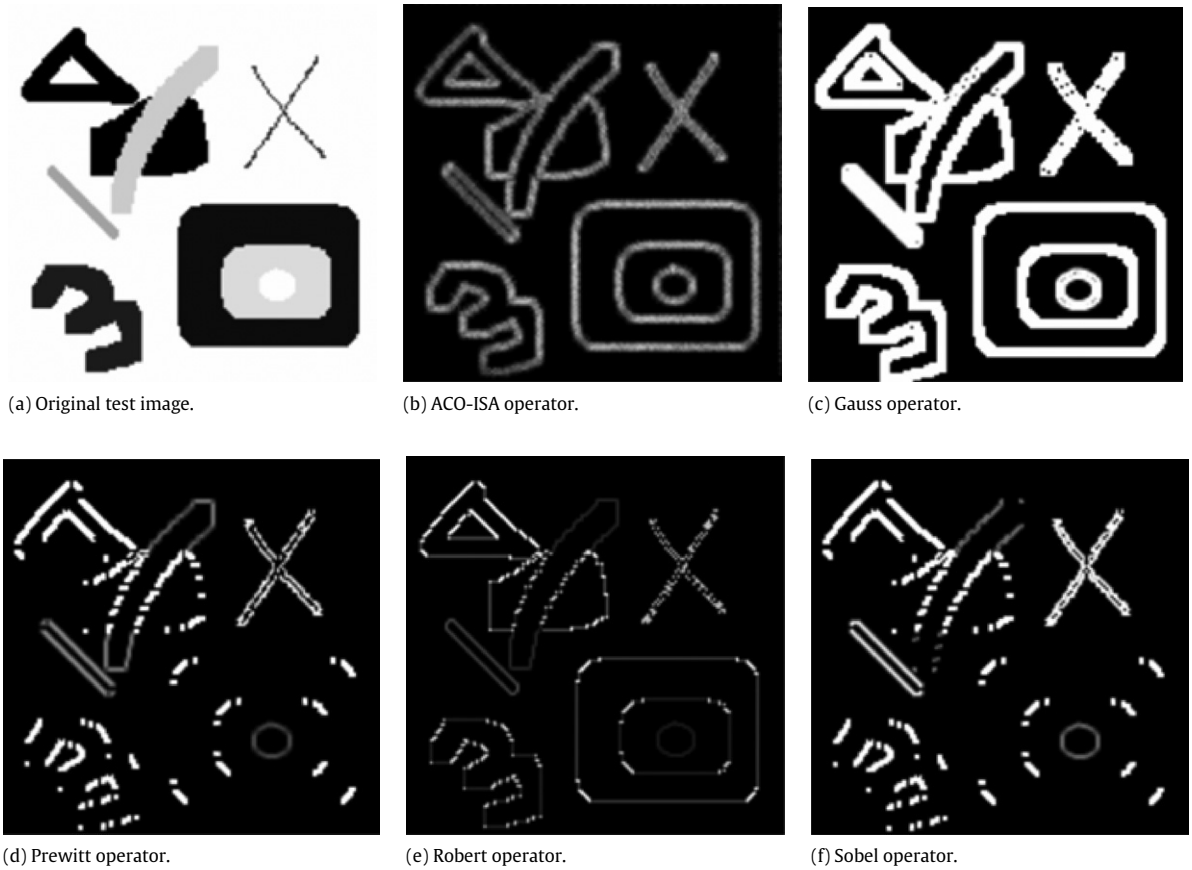

(a) Original test image. (b) ACO-ISA operator. (c) Gauss operator.

(d) Prewitt operator. (e) Robert operator. (f) Sobel operator.

Fig. 1. Comparison the performance of ACO-ISA with traditional edge detectors.

3.2.3. ACO based texture representation algorithm (ACO-TRA)

The procedure of this ACO based texture representation (which is named ACO-TRA) is slightly modified from ACO-ISA, and needs no detailed discussion here.

4. Experiments and results

In order to evaluate the performance of the proposed algorithms, we designed 3 experiments: the 1st one aimed at theoretically testing the performance of ACO-ISA and comparing with some traditional edge detectors; the 2nd one revealed the segmentation ability of ACO-ISA on iris images; and the 3rd one proved the capacity of the texture expression of ACO-TRA on iris disease focuses.

4.1. Testing the performance of ACO-ISA

First, to examine the performance of ACO-ISA, several test images were used. Throughout the experiment, the main parameters were set to the following values: the number of ants was set to 20% of the total number of pixels on an image; η was 0.3; K was 0.985; the maximum iteration was set to 200. These values seem to be appropriate for all the images, and could be changed with less effective difference in the quality of results. However, the other parameters were chosen according to different type of images, because they related closely with the histogram of different kinds of images. An example of the segmentation performance, together with comparison with traditional edge detectors, is given in Fig. 1.

4.2. ACO-ISA on iris images

Similarly, the performance of ACO-ISA is given in Fig. 2. It could be easily noted that the collarette and pigmentation regions are more instinct under the ACO-ISA detector, thus the ACO-ISA processed image would be a better bias for further applying region edging methods.

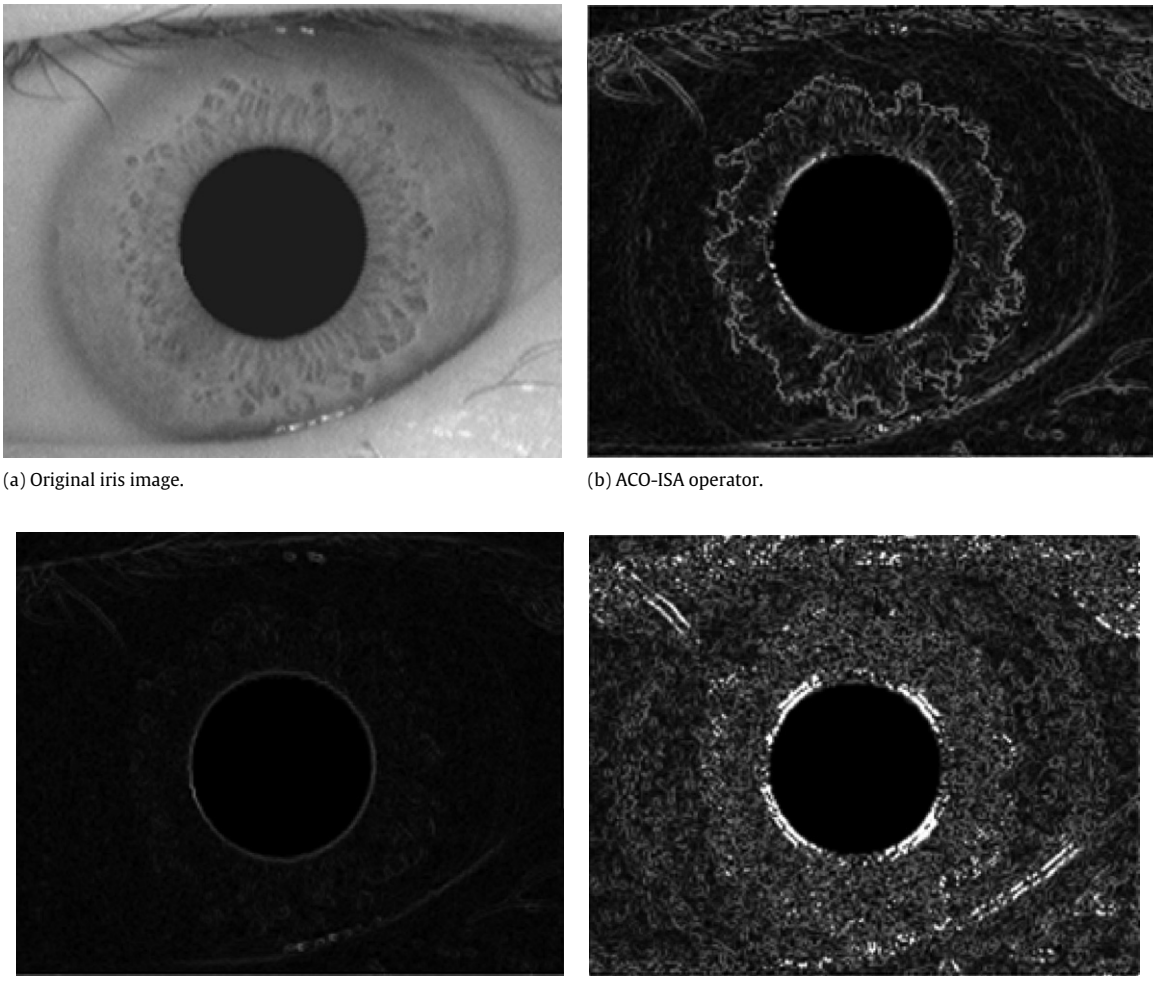

(a) Original iris image.

(b) ACO-ISA operator.

(c) Robert operator.

(d) Sobel operator.

Fig. 2. Performance of ACO-ISA on iris image.

Table 1
Inter-class distances between various iris regions.

Inter-class distance	*Hyper pigmentation*	*Radii solaris*	*Normal region*
Hyper pigmentation	/	13.55	84.41
Radii solaris	13.55	/	97.95
Normal region	84.41	97.95	/

4.3. Effect of ACO-TRA on iris images

In our 3rd experiments, the texture representation ability of ACO-TRA was tested on iris regions of 3 kinds of typical texture: normal texture, the texture of hyper pigmentations and the radii solaris. After ACO-TRA processing, each region was further aligned to 3×3 sub-zones, and the histogram for each sub-zone was then calculated. To compare 2 regions, the total distance was the mean of the histogram distances of all corresponding sub-zone pairs. In total, 900 example regions, 300 for each kind of texture, were involved in our experiment. The average inter-class distances are given in Table 1. Clearly, different texture regions could be well distinguished using our ACO representation. Furthermore, we also designed a self-organized feature map (SOFM) neural network as classifier for texture recognition, and a 93.9% of accurate recognition rate was achieved. This revealed that our method will be helpful in an automatic disease diagnosis system through iris images.

In our other experiments, tests were made on images with 2%, 4%, up to 10% Gaussian noise. From visual effects, the segmentation results were fairly good under noise up to 6%. Such results further proved that the proposed ACO based methods are quite promising.

5. Conclusion

In this paper, we described a novel approach to image segmentation and texture representation based on ACO. We proposed a framework for ACO based methods and created the flexibility of defining different mechanisms for an ant's behavior according to various problems. Each ant decides and acts depending on local information, but from the collective effect of the ant colony, the solution of the problem emerges. Experimental results proved that the ACO based methods are competitive with other traditional global optimization methods, extremely suitable for dealing with images with complex texture situations where local structural texture feature plays an important role.

References

[1] D.M. Cockburn, A study of the validity of iris diagnosis, Australian Journal of Optometry 64 (1981) 154–157.
[2] P. Knipschild, Looking for gall bladder disease in the patient's iris, British Medical Journal 297 (1988) 1578–1581.
[3] R.M. Haralick, Image segmentation survey, in: O.D. Faugeras (Ed.), Fundamentals in Computer Vision, Cambridge Univ. Press, Cambridge, 1983, pp. 209–224.
[4] B.S. Manjunath, R. Chellappa, Unsupervised texture segmentation using Markov random field models, IEEE Transactions on Pattern Analysis and Machine Intelligence 13 (5) (1991) 478–482.
[5] T.R. Reed, J.M.H. DuBuf, A review of recent texture segmentation and feature extraction techniques, CVGIP: Image Understanding 57 (3) (1993) 359–372.
[6] D. Dunn, W.E. Higgins, Optimal gabor filters for texture segmentation, IEEE Transactions on Image Processing 4 (7) (1995) 947–964.
[7] T. Hoffmann, J. Puzicha, J.M. Buhmann, Unsupervised texture segmentation in a deterministic annealing framework, IEEE Transactions on Pattern Analysis and Machine Intelligence 20 (8) (1998) 803–818.
[8] M. Unser, Texture classification and segmentation using wavelet frames, IEEE Transactions on Image Processing 4 (11) (1995) 1549–1560.
[9] T.P. Weldon, W.E. Higgins, An Algorithm for Designing Multiple Gabor Filters for Segmenting Multi-Textured Images, in: IEEE Int. Conf. Image Proc., Chicago, October 1998.
[10] C. Bouman, B. Liu, Multiple resolution segmentation of textured images, IEEE Transactions on Pattern Analysis and Machine Intelligence 13 (2) (1991) 99–113.
[11] H. Derin, H. Elliott, Modeling and segmentation of noisy and textured images using Gibbs random fields, IEEE Transactions on Pattern Analysis and Machine Intelligence 9 (1) (1987) 39–55.
[12] C. Kervrann, F. Heitz, A Markov random field model based approach to unsupervised texture segmentation using local and global spatial statistics, IEEE Transactions on Image Processing 4 (6) (1995) 856–862.
[13] B.S. Manjunath, R. Chellappa, Unsupervised texture segmentation using Markov random field models, IEEE Transactions on Pattern Analysis and Machine Intelligence 13 (5) (1991) 478–482.
[14] H.H. Nguyen, P. Cohen, Gibbs random fields, fuzzy clustering, and the unsupervised segmentation of textured images, CVGIP: Graph. Models and Image Processing 55 (1) (1993) 1–19.
[15] C.S. Won, H. Derin, Unsupervised segmentation of noisy and textured images using Markov random fields, CVGIP: Graphical Models and Image Processing 54 (4) (1992) 308–328.
[16] M. Dorigo, G.D. Caro, L.M. Gambardella, Ant algorithms for discrete optimization, Artificial Life 5 (2) (1999) 137–172.
[17] M. Dorigo, T. Stutzle, The ant colony optimization Meta-Heuristic: Algorithms, applications and advances, in: F. Glover, G. Kochenberger (Eds.), Handbook of Meta-heuristics, in: International Series in Operations Research & Management Science, vol. 57, Kluwer, Norwell, MA, 2002, pp. 251–285.
[18] L.U. Jue, An Self-Adaptive Ant Colony Optimization Approach for Image Segmentation, International Conference on Space Information Technology, 5985 (2005) pp.647–652.
[19] V. Ramos, F. Almeida, Artificial Ant Colonies in Digital Image Habitats—A mass Behavior Effect Study on Pattern Recognition, in: Proc. of 2nd Int. Wksp. on Ant Algorithms, Belgium, September 2000, pp. 113–116.
[20] C. Fernandes, V. Ramos, A.C. Rosa, Self-regulated artificial ant colonies on digital image habitats, International Journal of Lateral Computing 2 (1) (2005) 1–8.
[21] C. White, G. Tagliarini, S. Narayan, An algorithm for swarm based color image segmentation, in: Proc. IEEE Southeast Conf, IEEE Press, North Carolina, USA, 2004, pp. 84–89.
[22] X. Zhuang, N.E. Mastorakis, Image processing with the artificial swarm intelligence, WSEAS Transactions on Computers 4 (4) (2005) 333–341.
[23] L. Bocchi, L. Ballerini, S. Hassler, A new evolutionary algorithm for image segmentation, in: EuroGP'05 EvoWorkshops, in: LNCS series, Springer-Verlag, 2005.